Longitudinal Spin Structure of the Proton in Run Group C

Derek Holmberg 11-20-25

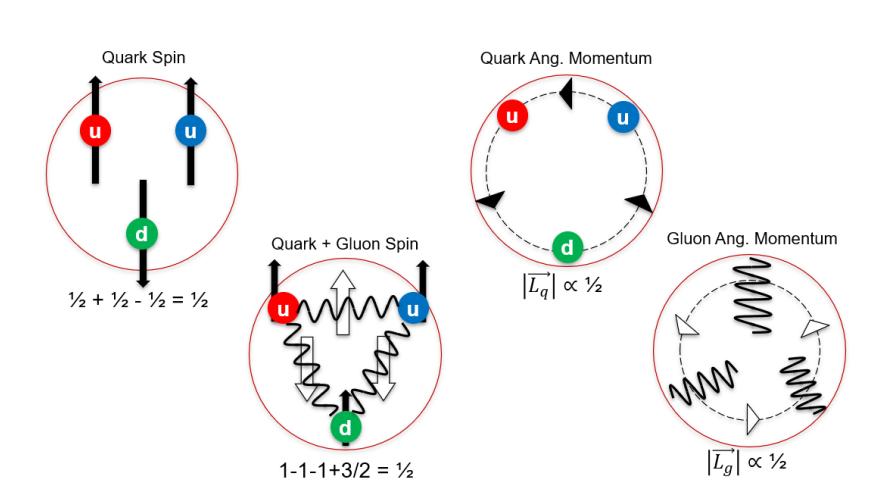


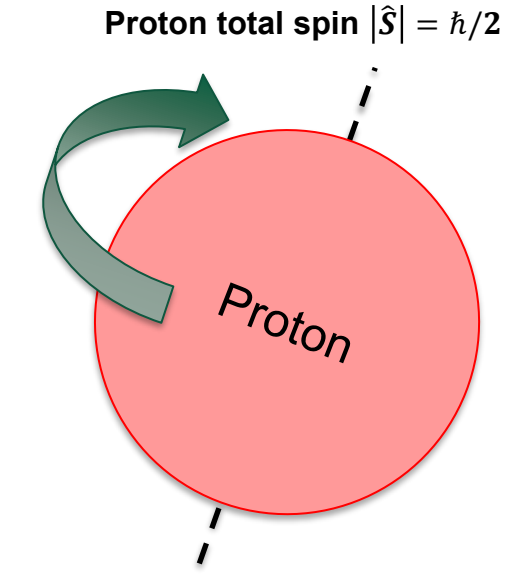




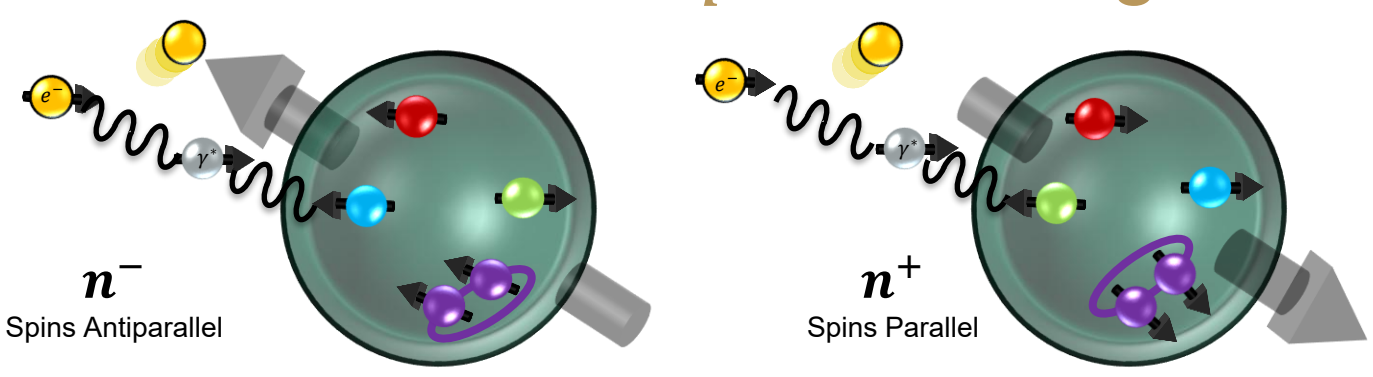
Where Does the Proton Spin Come From?

- Total proton spin $\frac{1}{2} = quark \ spin + gluon \ spin + quark \ orbital \ momentum + gluon \ orbital \ momentum$
- Quark spin contribution depends on polarized parton distribution functions (PDFs)
- Polarized PDF: $\Delta q_i(x) = q_i^{\uparrow}(x) q_i^{\downarrow}(x)$
- $g_1(x) \approx \frac{1}{2} \sum_i e_i^2 \Delta q_i(x) \propto \frac{1}{2} \left[\frac{4}{9} \Delta u(x) + \frac{1}{9} \Delta d(x) + \frac{1}{9} \Delta s(x) + \cdots \right]$
- Measure structure functions through polarized electron-proton scattering





Polarized ep Scattering



- Protons are polarized either parallel or antiparallel to the beam electrons' spins
- Deep inelastic scattering (DIS): electrons scatter off individual quarks ($Q^2 > 1 \text{ GeV}^2$, W > 2 GeV)
- Scattering conserves spin (angular momentum), so any asymmetry between n^{\pm} is related to spin structure

$$A_{||}(x,Q^2) = \frac{n^- - n^+}{n^- + n^+} = D(A_1(x,Q^2) + \eta A_2(x,Q^2))$$

• With A_1 , A_2 = virtual photon asymmetries

$$A_1(x, Q^2) \propto \frac{g_1(x, Q^2)}{F_1(x, Q^2)} \approx \frac{\sum_i e_i^2 \Delta q_i(x, Q^2)}{\sum_i e_i^2 q_i(x, Q^2)}$$

Run Group C Experimental Setup

- Ran from June 2022 to March 2023 for 80 PAC days (120 scheduled)
- RG-C data divided into five run periods:
 - Summer 2022: Inbending (Negative Solenoid and Torus)
 - Runs 16128 16772
 - Fall 2022: Inbending (Negative Solenoid and Torus)
 - Runs 16859 17183
 - Fall 2022: Inbending (Positive Solenoid, Negative Torus)
 - Runs 17188 17408
 - Spring 2023: Inbending (Negative Solenoid and Torus)
 - Runs 17482 17768
 - Spring 2023: Outbending (Negative Solenoid, Positive Torus)
 - Runs 17769 17811
- Used several target types:
 - Frozen ammonia targets: NH3 for protons, ND3 for deuterons
 - Carbon foil targets
 - Polyethylene (and deuterated polyethylene) foil targets
 - Empty targets (both filled with liquid helium and completely empty)

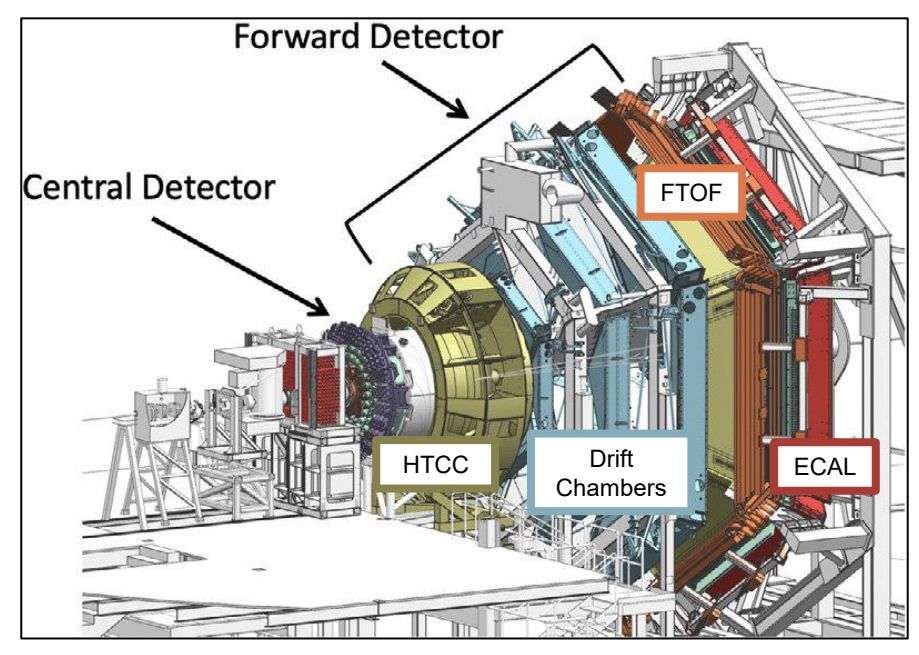


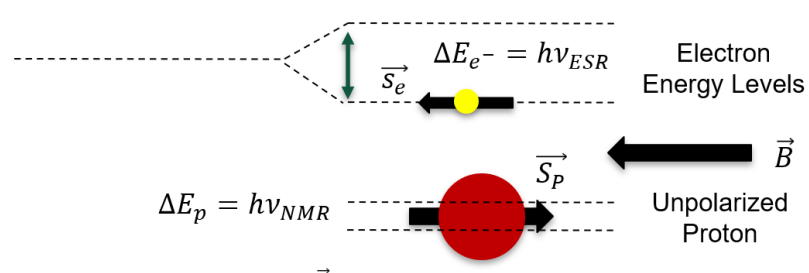
Diagram of CLAS12 Detector, Ziegler et. al.

• Generate polarized protons (deuterons) with RG-C polarized target

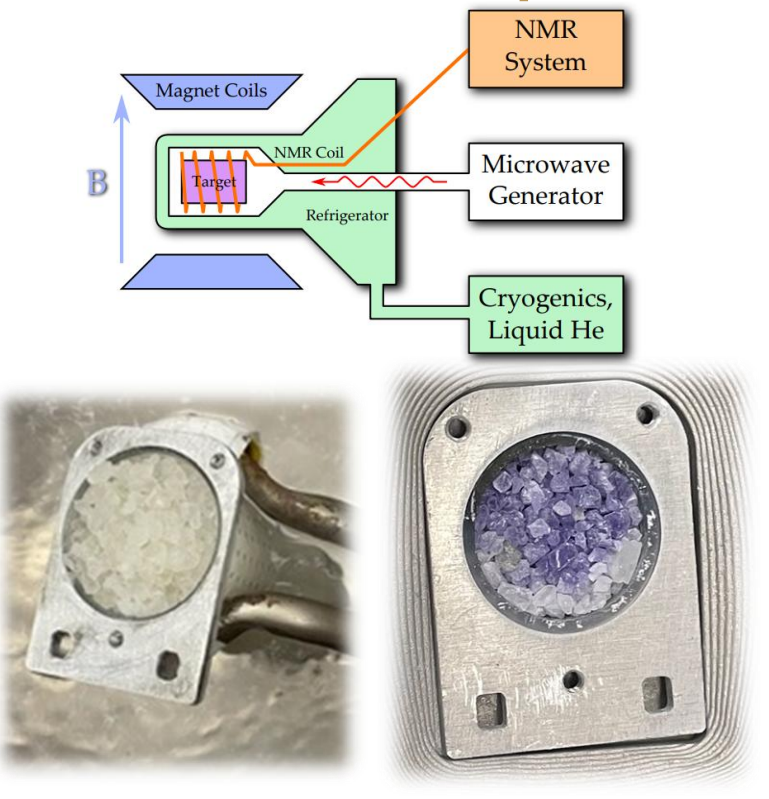
Run Group C Experimental Setup

- Generate polarized protons (deuterons) with RG-C polarized target
- Ammonia crystals, polarized via dynamic nuclear polarization (DNP)
- Cool to ~1 K in a 5 T field generated by solenoid, where free electrons almost completely polarize
- Using microwaves with a frequency of $v_{ESR} \pm v_{NMR}$ (~140 GHz), transfer electron polarization to the protons (or deuterons)
- ~90% for protons, ~40% for deuterons

 \vec{B} -field polarizes e^- , splits energy levels



 \vec{B} -field splits proton energy levels



Ammonia crystals unexposed to beam (left), crystals after beam exposure (right). Purple color from paramagnetic centers. 5

Electron PID Cuts

- Inclusive electron scattering: $ep \rightarrow eX$, $ed \rightarrow eX$
- Forward Detector: DC, ECAL, HTCC
- Electron Event Builder PID:
 - Negative track in the DC
 - $E_{PCAL} > 60 \text{ MeV}$
 - Photoelectrons in HTCC nphe > 2
- Deep inelastic kinematic cuts:
 - $Q^2 > 1 \text{ GeV}^2, W > 2 \text{ GeV},$
 - E' > 2.6 GeV (minimize radiative effects)
- Fiducial cuts (work in progress):
 - Summer: $-9 \text{ cm} < V_Z < 1 \text{ cm}, |V_{X,Y}| < 2 \text{ cm}$
 - Fall & Spring: $-7.5 \text{ cm} < V_Z < 2.5 \text{ cm}, |V_{X,Y}| < 2 \text{ cm}$
 - 5° < θ < 40°, $|\chi^2_{PID}|$ < 3
 - Region-dependent drift chamber edge cuts:
 - EdgeR1 > 4 cm, EdgeR2 > 5 cm, EdgeR3 > 8 cm
 - Working on ECAL fiducial cuts based on L-strips
 - PCAL Lv, Lw > 9 cm (based on RG-A fiducial studies)
- QADB cuts for all run periods

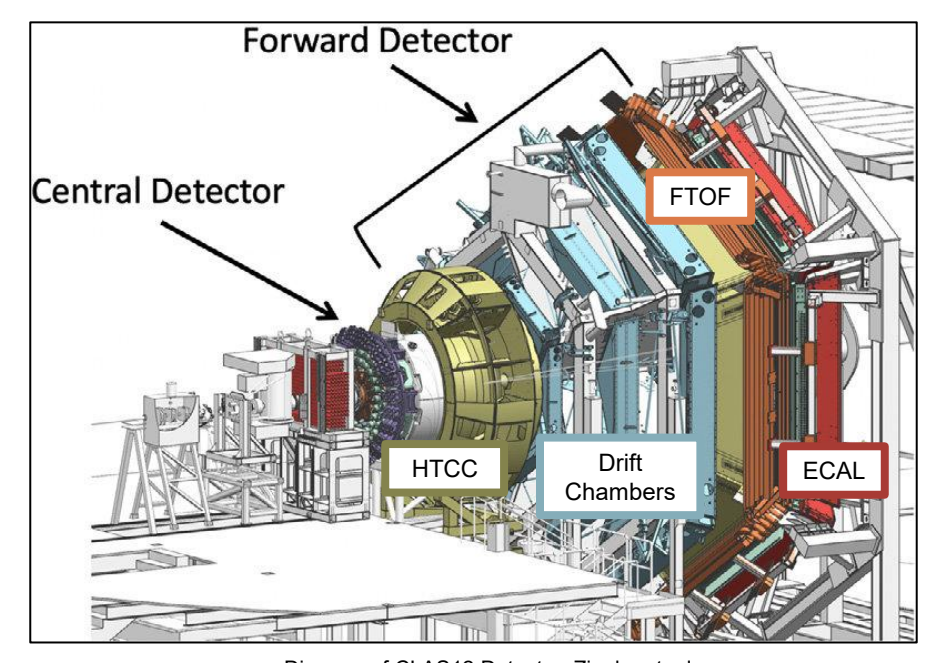
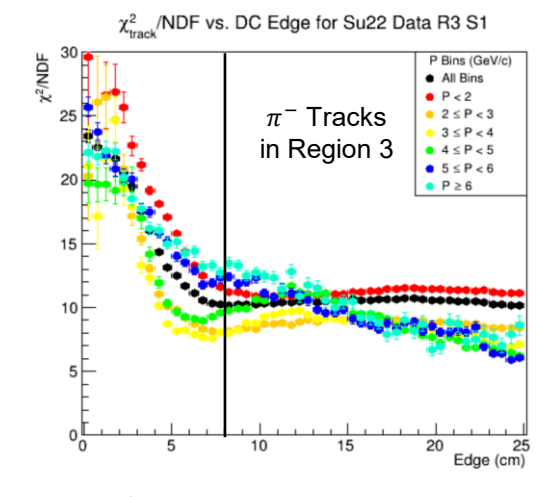
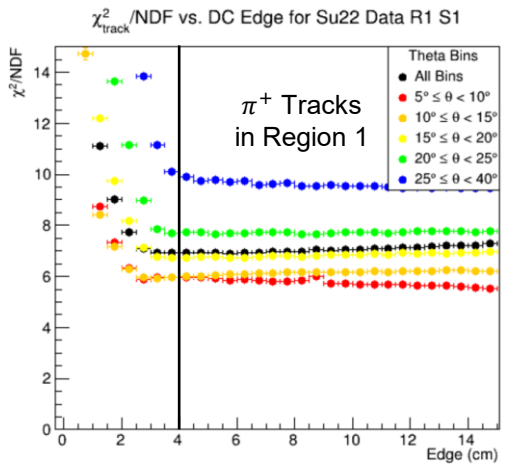


Diagram of CLAS12 Detector, Ziegler et. al.

Electron PID Cuts

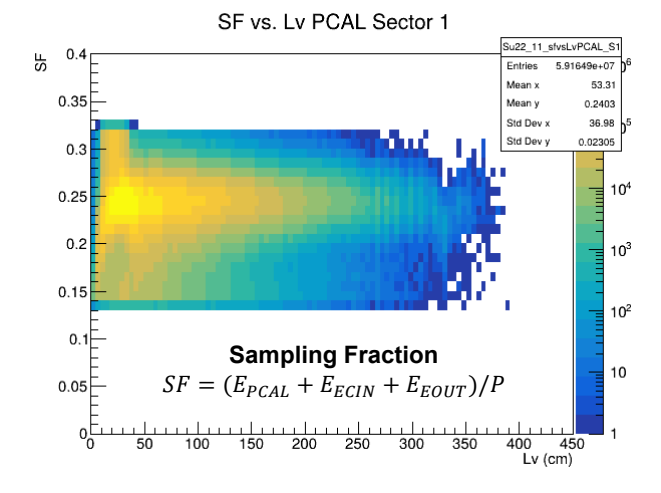
- Inclusive electron scattering: $ep \rightarrow eX$, $ed \rightarrow eX$
- Forward Detector: DC, ECAL, HTCC
- Electron Event Builder PID:
 - Negative track in the DC
 - $E_{PCAL} > 60 \text{ MeV}$
 - Photoelectrons in HTCC nphe > 2
- Deep inelastic kinematic cuts:
 - $Q^2 > 1 \text{ GeV}^2, W > 2 \text{ GeV},$
 - E' > 2.6 GeV (minimize radiative effects)
- Fiducial cuts (work in progress):
 - Summer: $-9 \text{ cm} < V_Z < 1 \text{ cm}, |V_{X,Y}| < 2 \text{ cm}$
 - Fall & Spring: $-7.5 \text{ cm} < V_Z < 2.5 \text{ cm}, |V_{X,Y}| < 2 \text{ cm}$
 - 5° < θ < 40°, $|\chi^2_{PID}|$ < 3
 - Region-dependent drift chamber edge cuts:
 - EdgeR1 > 4 cm, EdgeR2 > 5 cm, EdgeR3 > 8 cm
 - Working on ECAL fiducial cuts based on L-strips
 - PCAL Lv, Lw > 9 cm (based on RG-A fiducial studies)
- QADB cuts for all run periods

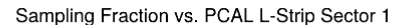


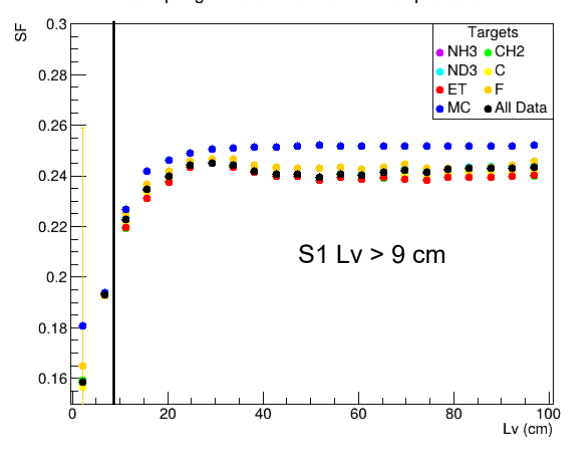


Electron PID Cuts

- Inclusive electron scattering: $ep \rightarrow eX$, $ed \rightarrow eX$
- Forward Detector: DC, ECAL, HTCC
- Electron Event Builder PID:
 - Negative track in the DC
 - $E_{PCAL} > 60 \text{ MeV}$
 - Photoelectrons in HTCC nphe > 2
- Deep inelastic kinematic cuts:
 - $Q^2 > 1 \text{ GeV}^2, W > 2 \text{ GeV},$
 - E' > 2.6 GeV (minimize radiative effects)
- Fiducial cuts (work in progress):
 - Summer: $-9 \text{ cm} < V_Z < 1 \text{ cm}, |V_{X,Y}| < 2 \text{ cm}$
 - Fall & Spring: $-7.5 \text{ cm} < V_Z < 2.5 \text{ cm}, |V_{X,Y}| < 2 \text{ cm}$
 - 5° < θ < 40°, $|\chi^2_{PID}|$ < 3
 - Region-dependent drift chamber edge cuts:
 - EdgeR1 > 4 cm, EdgeR2 > 5 cm, EdgeR3 > 8 cm
 - Working on ECAL fiducial cuts based on L-strips
 - PCAL Lv, Lw > 9 cm (based on RG-A fiducial studies)
- QADB cuts for all run periods







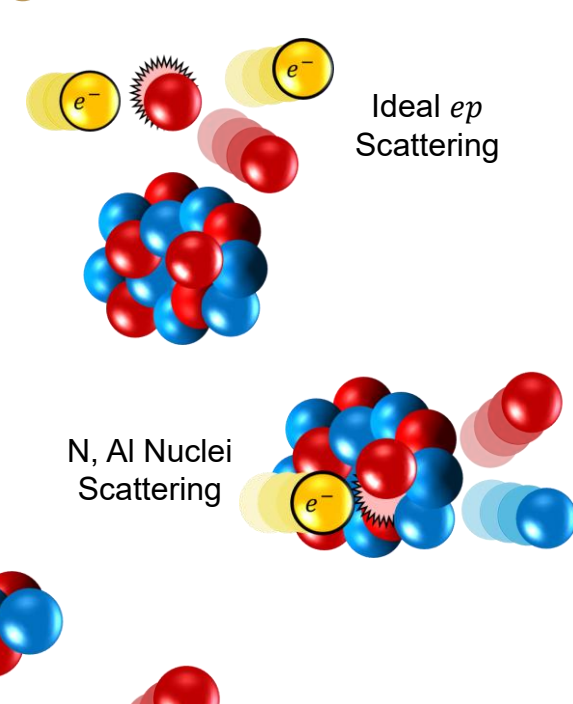
Unpolarized Background and Beam-Target Polarization

- Unpolarized background: N, Al, He nuclei in target/bath
- Reduces measured A_{II} , and cannot be removed with vertex/kinematic cuts
- Quantified using a dilution factor D_F

$$D_F = \frac{Y_H}{Y_{Ammonia}} = \frac{3\sigma_H \ell_H \rho_H}{(3\sigma_H + \sigma_N)\ell_A \rho_A + \sigma_{He} \ell_{He} \rho_{He} + \sigma_{Al} \ell_{Al} \rho_{Al}}$$

- Imperfect polarization of beam electrons and target particles: $P_b P_t$
- Dividing $A_{||}$ by D_F and P_bP_t accounts for the background

$$A_{||,phys} = \frac{A_{||,raw}}{D_F P_b P_t} \propto A_1$$



Unpolarized Background and Beam-Target Polarization

- Unpolarized background: N, Al, He nuclei in target/bath
- Reduces measured $A_{||}$, and cannot be removed with vertex/kinematic cuts
- Quantified using a dilution factor D_F

$$D_F = \frac{Y_H}{Y_{Ammonia}} = \frac{3\sigma_H \ell_H \rho_H}{(3\sigma_H + \sigma_N)\ell_A \rho_A + \sigma_{He} \ell_{He} \rho_{He} + \sigma_{Al} \ell_{Al} \rho_{Al}}$$

- Imperfect polarization of beam electrons and target particles: P_bP_t
- Dividing $A_{||}$ by D_F and P_bP_t accounts for the background

$$A_{||,phys} = \frac{A_{||,raw}}{D_F P_b P_t} \propto A_1$$

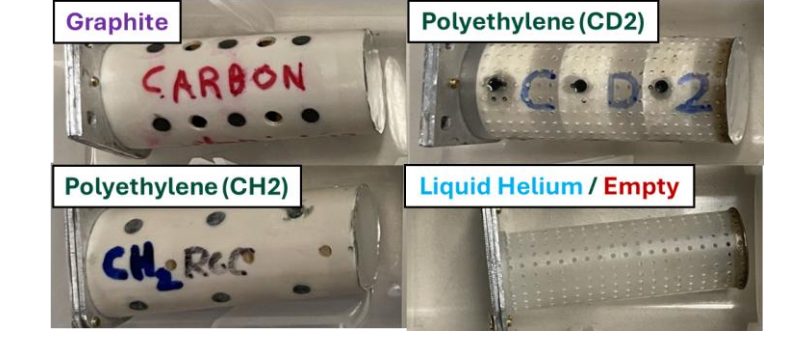


Beam Electron Polarization P_h



Calculating the Dilution Factor

- Advantageous to write D_F in terms of scattering counts from background targets instead of cross sections
- Counts from the targets are functions of the cross sections
- Using information from all targets, write the yields in terms of scattering counts
- $n_A(\sigma_{Al}, \sigma_{He}, \sigma_C, \sigma_H)$, where $\frac{7}{6}\sigma_C \approx \sigma_N$
- $n_{MT}(\sigma_{Al}, \sigma_{He}), \quad n_{C}(\sigma_{Al}, \sigma_{He}, \sigma_{C})$
- $n_{CH}(\sigma_{Al}, \sigma_{He}, \sigma_{C}, \sigma_{H}), n_{F}(\sigma_{Al})$



Solving for the yields and rewriting the D_F:

$$D_F(x, Q^2) = P_F \frac{C_1 n_C + C_2 n_{MT} + C_3 n_{CH} + C_4 n_F}{C_5 n_A}$$

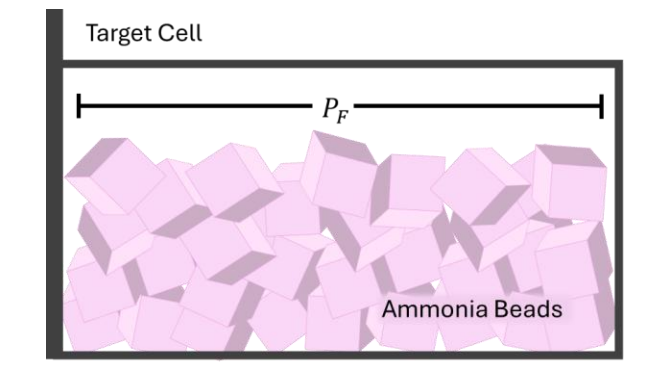
• Packing fraction P_F is the target volume fraction occupied by the ammonia crystals

$$P_F(x,Q^2) = \frac{D_1(n_A - n_{MT})}{D_2 n_{MT} + D_3 n_C + D_4 n_{CH} + D_5 n_F}$$

 C_i , $D_i \propto \ell_i$, ρ_i of target materials

Calculating the Dilution Factor

- Advantageous to write D_F in terms of scattering counts from background targets instead of cross sections
- Counts from the targets are functions of the cross sections
- Using information from all targets, write the yields in terms of scattering counts
- $n_A(\sigma_{Al}, \sigma_{He}, \sigma_C, \sigma_H)$, where $\frac{7}{6}\sigma_C \approx \sigma_N$
- $n_{MT}(\sigma_{Al}, \sigma_{He}), \quad n_{C}(\sigma_{Al}, \sigma_{He}, \sigma_{C})$
- $n_{CH}(\sigma_{Al}, \sigma_{He}, \sigma_{C}, \sigma_{H}), n_{F}(\sigma_{Al})$



Solving for the yields and rewriting the D_F:

$$D_F(x,Q^2) = P_F \frac{C_1 n_C + C_2 n_{MT} + C_3 n_{CH} + C_4 n_F}{C_5 n_A}$$

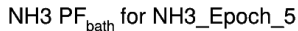
• Packing fraction P_F is the target volume fraction occupied by the ammonia crystals

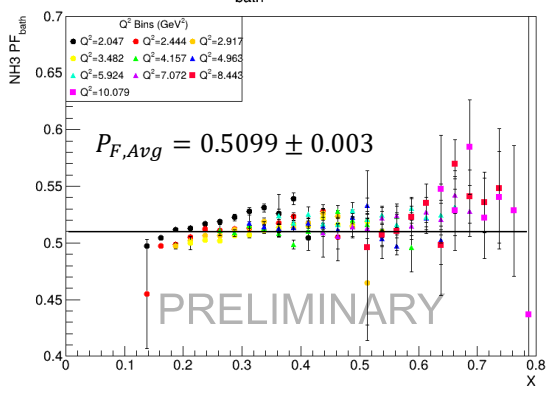
$$P_F(x,Q^2) = \frac{D_1(n_A - n_{MT})}{D_2 n_{MT} + D_3 n_C + D_4 n_{CH} + D_5 n_F}$$

 C_i , $D_i \propto \ell_i$, ρ_i of target materials

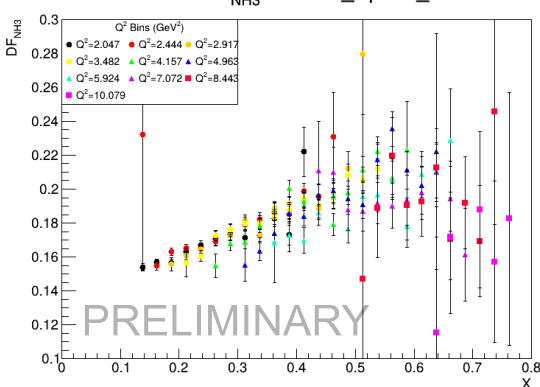
Calculating the Dilution Factor

- Two methods are used to calculate the dilution factor: a data-driven method and a model of the dilution factor
- Data-driven method:
 - Measure $n_A n_{MT} n_C n_{CH} n_F$ from the data
 - Use these values to calculate a value of P_F for each x, Q^2 bin
 - Calculate a weighted average of all P_F
 - Use this $P_{F,avg}$ as an input to calculate D_F for each x, Q^2 bin
 - Requires a radiation length correction to empty n_{MT} and foil n_F counts (haven't found a suitable model yet)
- Modeled dilution factor:
 - From modeled structure functions, "build" each target and simulate the counts $n_A n_{MT} n_C n_{CH} n_F$ coming from the target
 - Accounts for EMC effect, fermi motion, and radiative corrections to be built-in to the model
 - Helps estimate D_F in low-statistics regions
 - Model is tuned to fit experimentally measured D_F and P_F





NH3 DF_{NH3} for NH3_Epoch_5



- Calculated preliminary D_F for the RGC dataset
- Datasets are broken up into different "epochs" that have different packing fractions
- D_E binned in x for each epoch
- Once D_F are calculated, use them to get P_hP_t

Summer 2022 Runs

Epoch 2: Runs 16137 – 16178 Epoch 3: Runs 16211 – 16260 Epoch 4: Runs 16318 – 16357 Epoch 5: Runs 16658 – 16674 Epoch 6: Runs 16675 – 16695 Epoch 7: Runs 16709 – 16732 Epoch 8: Runs 16742 – 16752 Epoch 9: Runs 16753 – 16766 Epoch 10: Runs 16767 – 16772

Χ

Fall 2022 Runs

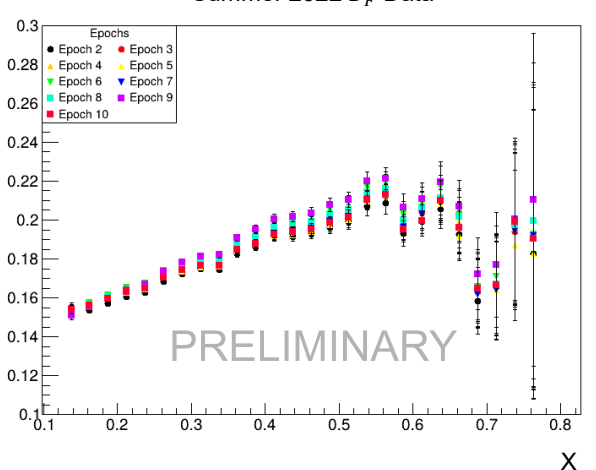
Epoch 11: Runs 16983 – 16993 Epoch 12: Runs 16695 – 17032 Epoch 13: Runs 17067 – 17102 Epoch 14: Runs 17144 – 17161 Epoch 15: Runs 17162 – 17169 Epoch 16: Runs 17188 – 17214 Epoch 17: Runs 17215 – 17225 Epoch 18: Runs 17353 – 17368

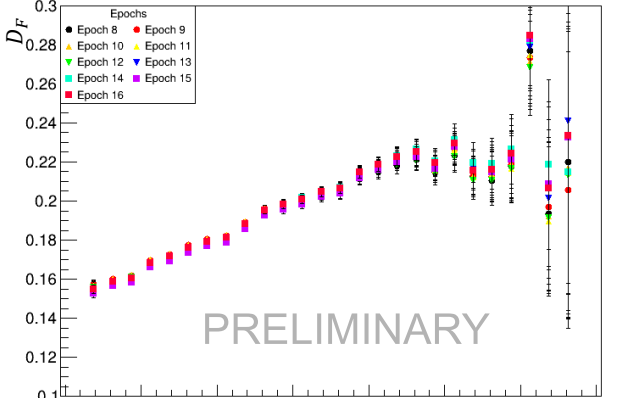
Epoch 19: Runs 17371 – 17382

Spring 2023 Runs

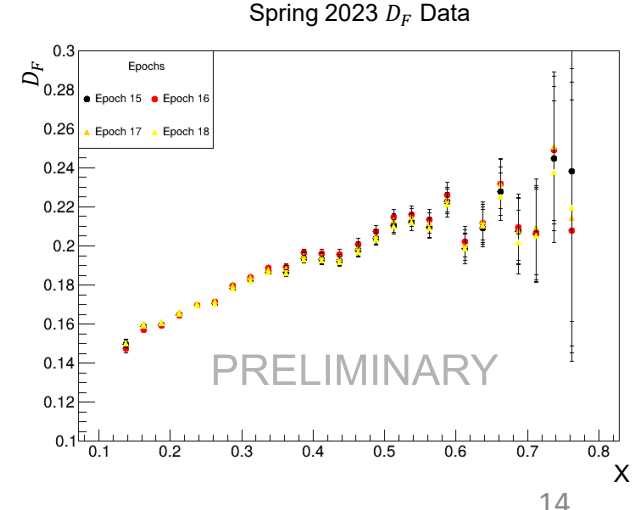
Epoch 20: Runs 17575 – 17597 Epoch 21: Runs 17598 – 17611 Epoch 22: Runs 17720 – 17741 Epoch 23: Runs 17748 – 17762 Epoch 24: Runs 17769 – 17778 (Epoch 24 is outbending)

Summer 2022 D_F Data





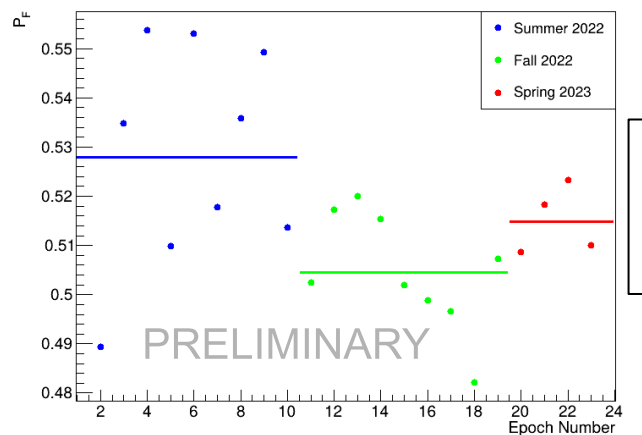
Fall 2022 D_F Data



Packing Fractions for RG-C Epochs

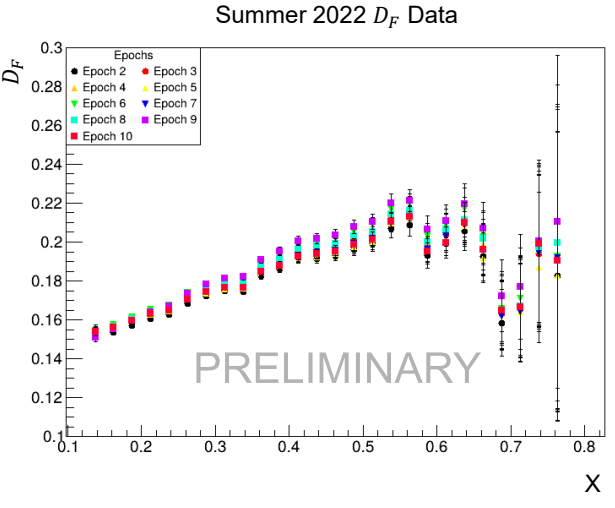
Preliminary Results

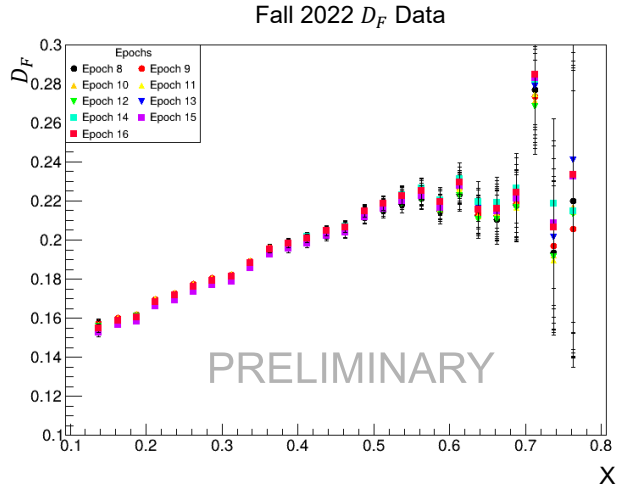
- P Calculated preliminary D_F for the RGC dataset
- Datasets are broken up into different "epochs" that have different packing fractions
- D_F binned in x for each epoch
- Once D_F are calculated, use them to get P_hP_t

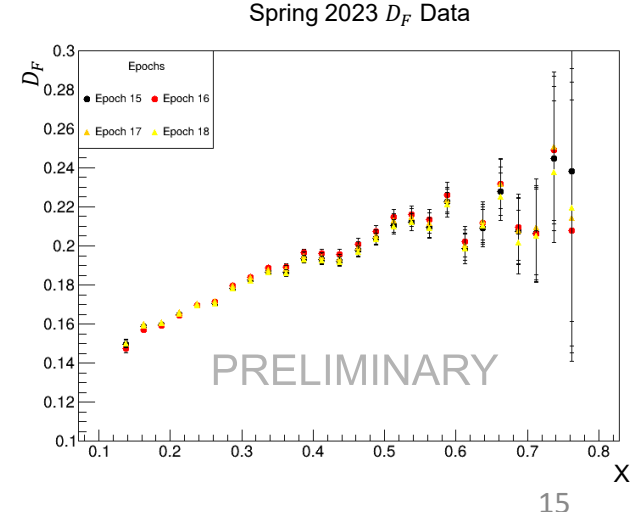


Weighted Average P_F Per Run Period:

Summer 2022 $P_F = 0.5280 \pm 0.0001$ Fall 2022 $P_F = 0.5045 \pm 0.0001$ Spring 2023 $P_F = 0.5149 \pm 0.0001$







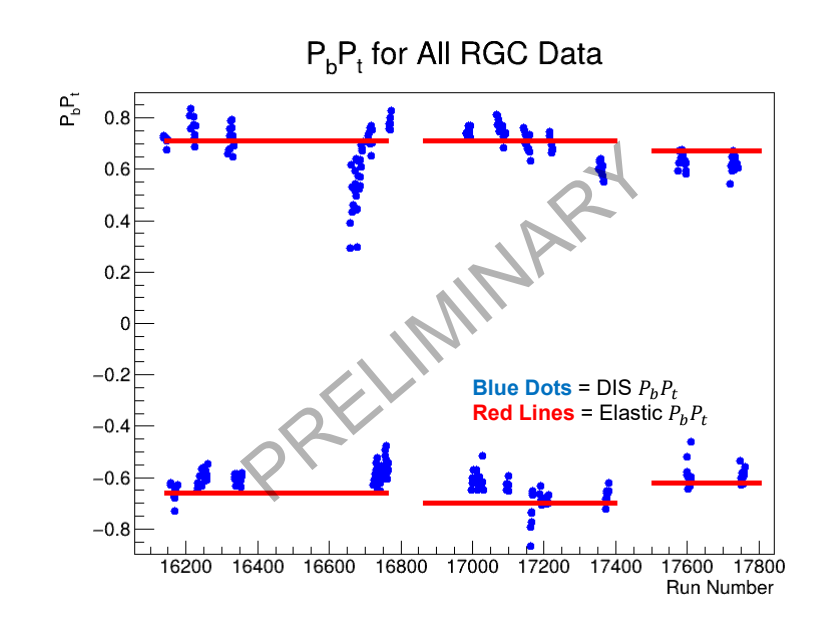
Beam-Target Polarization Calculations

$$A_{||,phys} = \frac{A_{||,raw}}{D_F P_b P_t} \quad \Rightarrow \quad P_b P_t = \frac{A_{||,raw}}{D_F A_{||,phys}}$$

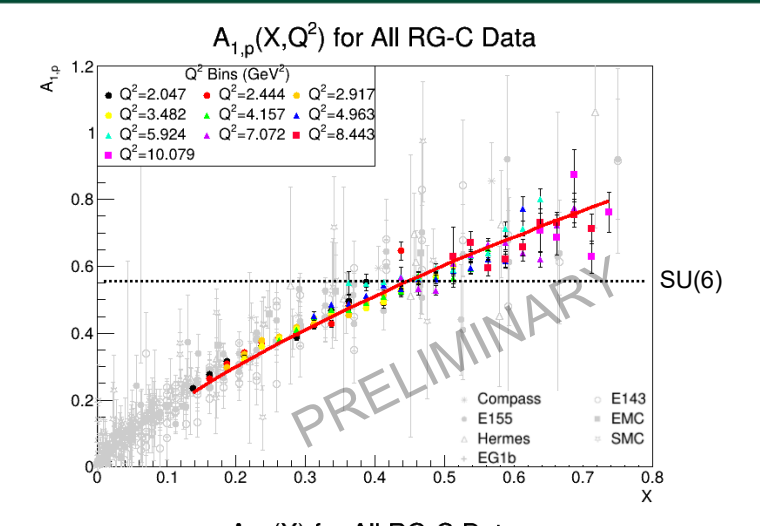
- Use a model to calculate A_{||,phys}
- For DIS $P_b P_t$, calculated over x, Q^2 bins using $A_{th} = D(A_1 + \eta A_2)$, with values of D, η , A_1 , A_2 come from S. Kuhn 's model
- Model is a parameterized fit to existing world data
- Calculated through the maximum likelihood method:

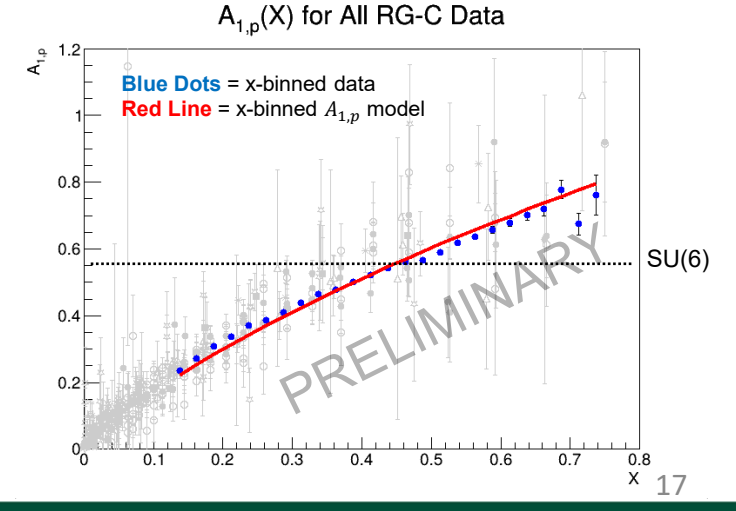
$$P_b P_t = \frac{\sum_{x,Q^2 \ bins} D_{F,i} A_{th,i} (n_i^- - n_i^+)}{\sum_{x,Q^2 \ bins} D_{F,i}^2 A_{th,i}^2 (n_i^- + n_i^+)}$$

- Values of $P_b P_t$ were also calculated for RGC data using exclusive elastic $ep \rightarrow e'p'$ scattering (Noemie Pilleux)
- Elastic asymmetry parameterized by Arrington et. al.
- Normalize DIS $P_b P_t$ to elastic $P_b P_t$ using $f \sim P_b P_{telastic} / P_b P_{tols,ava}$
- However, since there are corrections required for both DIS and Elastic (polarized nitrogen, D_F normalization, etc.), the results shown for $A_{1,p}$ will use just the DIS results from this slide

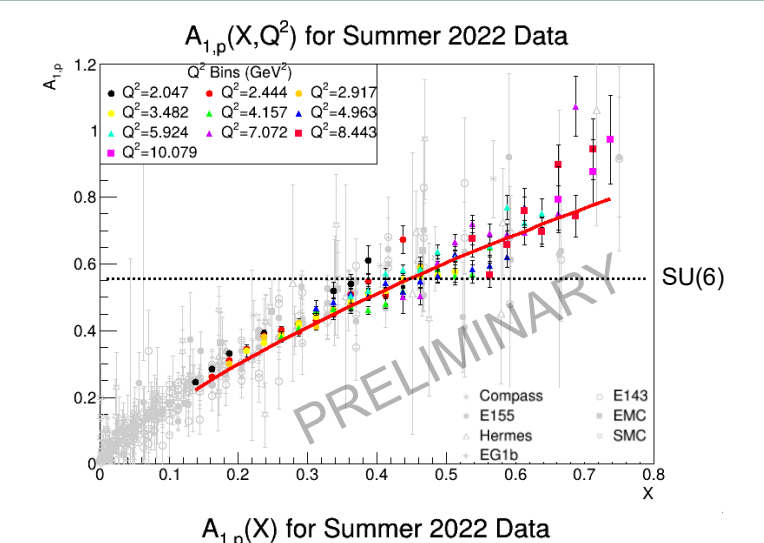


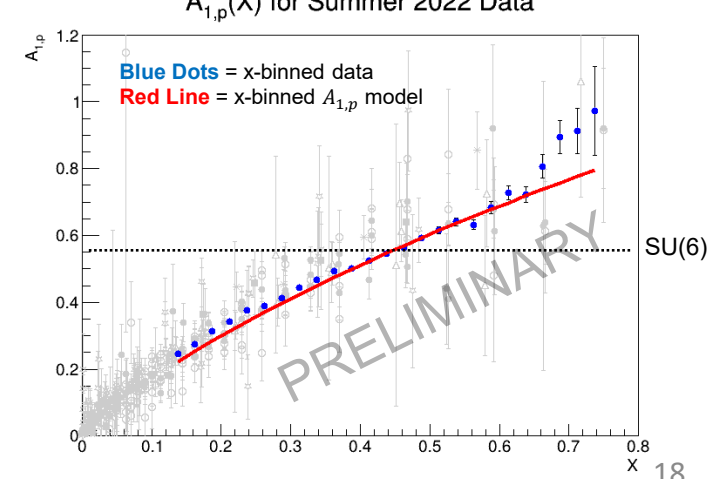
- To calculate $A_{1,p}$, rearrange $A_{\parallel,phys} = D(A_1 + \eta A_2)$
- $A_1 = A_{\parallel,phys}/D \eta A_2$, with D, η , A_2 from S. Kuhn's model
- Values of η , A_2 are small for DIS kinematics, so smaller effects from model
- Spring 2023 data excludes outbending runs
- Data fluctuates around model values of A_{1,p}
- Currently, we don't have data-driven $A_{1,d}$ results due to issues with calculating the ND3 D_F



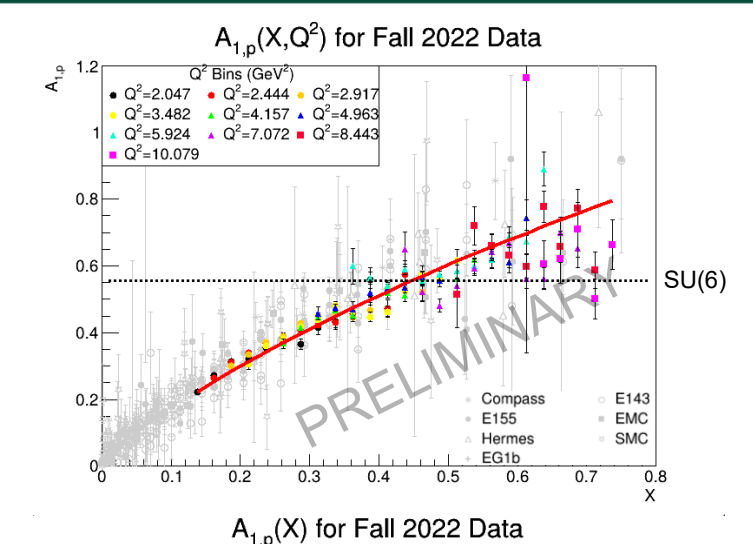


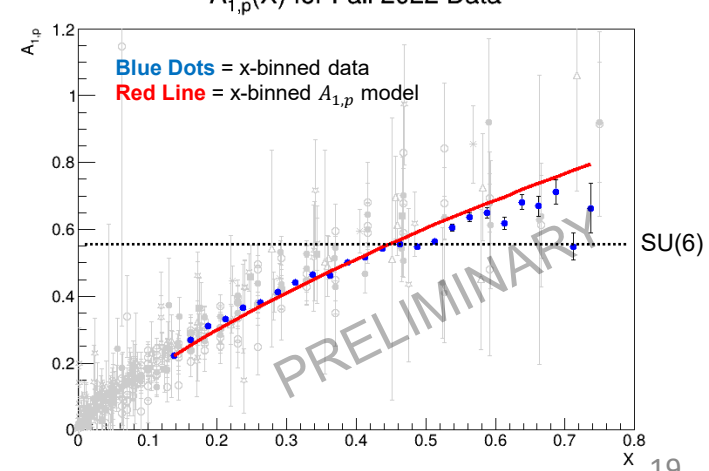
- To calculate $A_{1,p}$, rearrange $A_{\parallel,phys} = D(A_1 + \eta A_2)$
- $A_1 = A_{\parallel,phys}/D \eta A_2$, with D, η , A_2 from S. Kuhn's model
- Values of η , A_2 are small for DIS kinematics, so smaller effects from model
- Spring 2023 data excludes outbending runs
- Data fluctuates around model values of $A_{1,p}$
- Currently, we don't have data-driven $A_{1,d}$ results due to issues with calculating the ND3 D_F



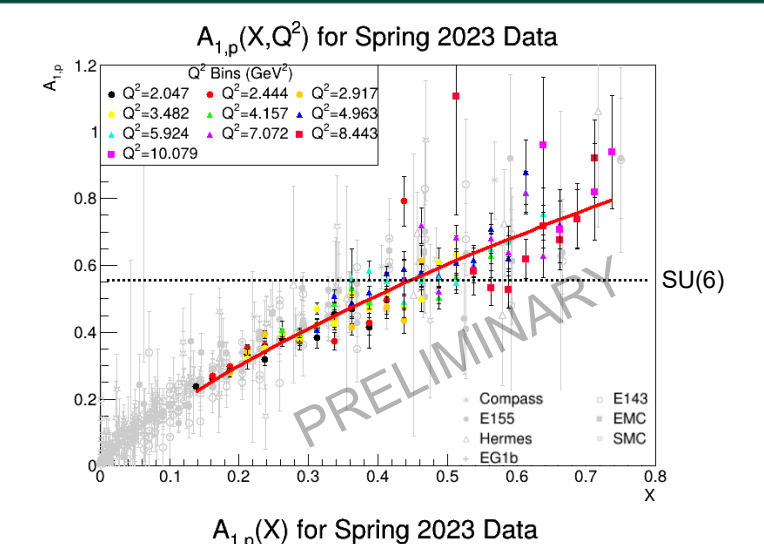


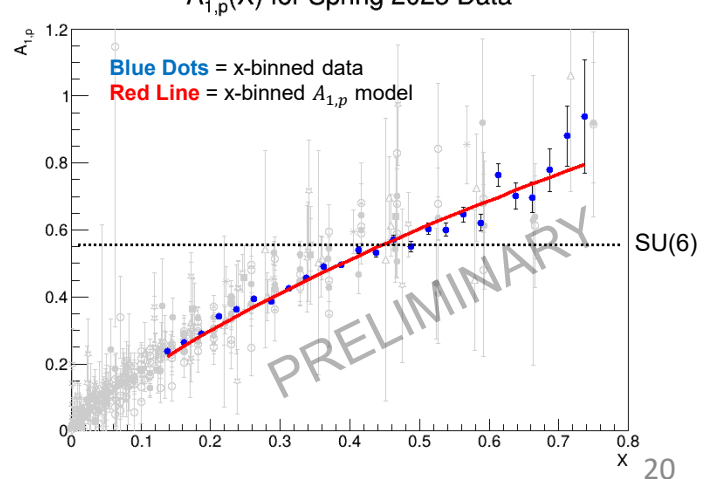
- To calculate $A_{1,p}$, rearrange $A_{\parallel,phys} = D(A_1 + \eta A_2)$
- $A_1 = A_{\parallel,phys}/D \eta A_2$, with D, η , A_2 from S. Kuhn's model
- Values of η , A_2 are small for DIS kinematics, so smaller effects from model
- Spring 2023 data excludes outbending runs
- Data fluctuates around model values of A_{1,p}
- Currently, we don't have data-driven $A_{1,d}$ results due to issues with calculating the ND3 D_F





- To calculate $A_{1,p}$, rearrange $A_{\parallel,phys} = D(A_1 + \eta A_2)$
- $A_1 = A_{\parallel,phys}/D \eta A_2$, with D, η , A_2 from S. Kuhn's model
- Values of η , A_2 are small for DIS kinematics, so smaller effects from model
- Spring 2023 data excludes outbending runs
- Data fluctuates around model values of A_{1,p}
- Currently, we don't have data-driven $A_{1,d}$ results due to issues with calculating the ND3 D_F

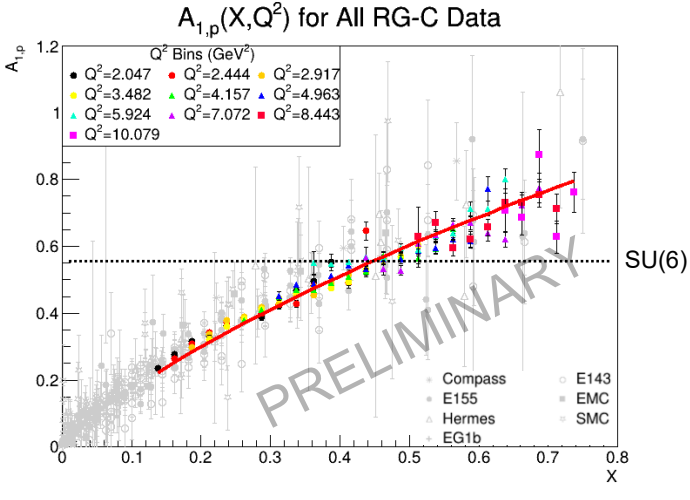




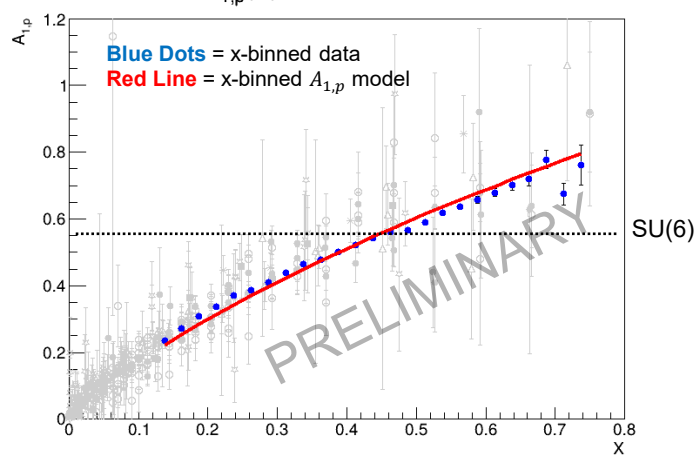
Work Left To Do

- Incorporate radiation length corrections to n_{MT} , n_F counts
- Correct $P_b P_t$ for polarized ¹⁴N in target
- Finalize the D_F model-driven approach
- Finalize ECAL fiducial cuts and implement sampling fraction (SF) vs. momentum cuts

Any Questions?





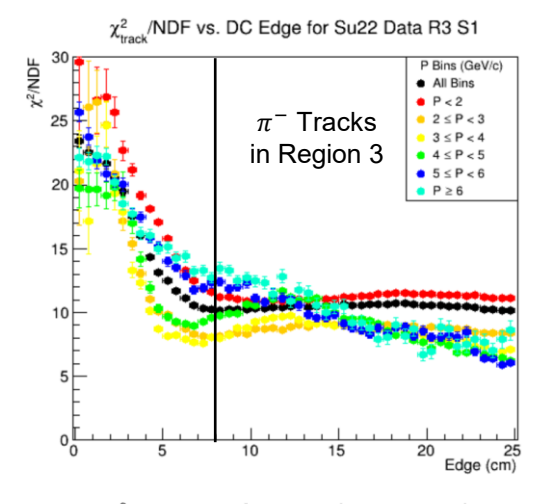


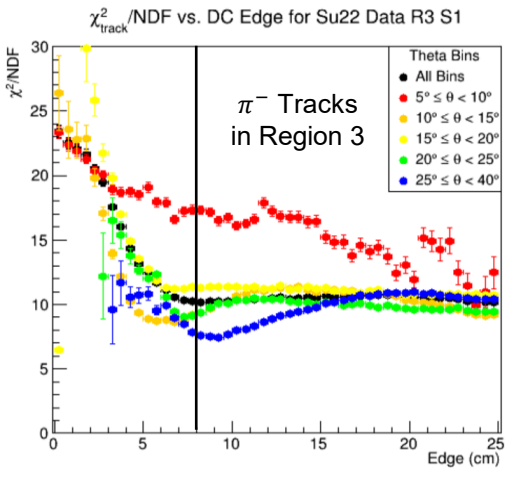
Backup Slides

- DC and ECAL fiducial cuts
- Thermal expansion corrections to targets
- All D_F and P_F for NH3 targets across all x, Q^2 bins
- All D_F and P_F for ND3 targets across all x, Q^2 bins

Determining Cuts For DC

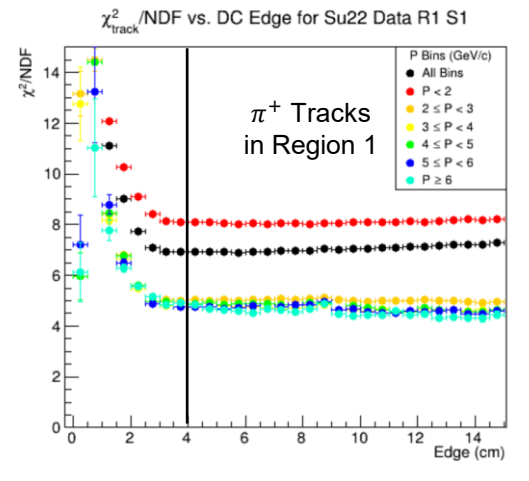
- The DC fiducial cuts based on average χ^2_{track}/NDF vs. edge variable of track
- Cuts selected qualitatively based on where average χ^2 rises relative to the rest of the distribution
- Analyzed separately for inbending and outbending data using π^+, π^-
- Tracks binned in polar scattering angle θ , momentum P
- Iterative procedure for making cuts:
 - First, make cuts for Region 3 using inbending data and cuts for Region 1 using outbending data
 - 2. After Region 1 and 3 cuts are applied, look at Region 2 and make cuts for inbending and outbending
- Checked for each sector in each region
- No momentum, θ -dependent cuts
- Vertex cuts applied
 - Summer 2022: $-9 \text{ cm} \le V_Z \le 1 \text{ cm}, |V_{X,Y}| < 2 \text{ cm}$
 - Fall 2022 & Spring 2023: -7.5 cm ≤ V_Z ≤ 2.5 cm, $|V_{X,Y}|$ < 2 cm

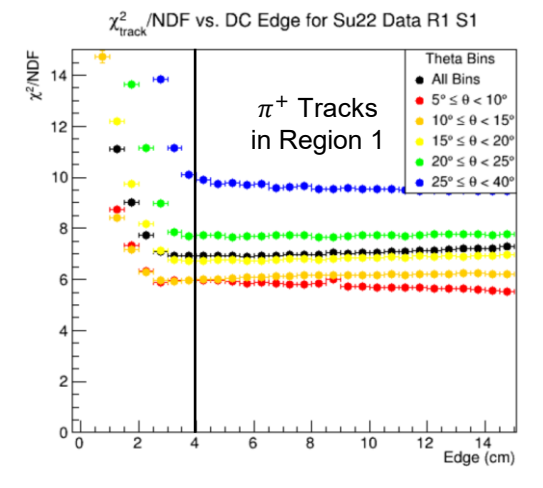




Determining Cuts For DC

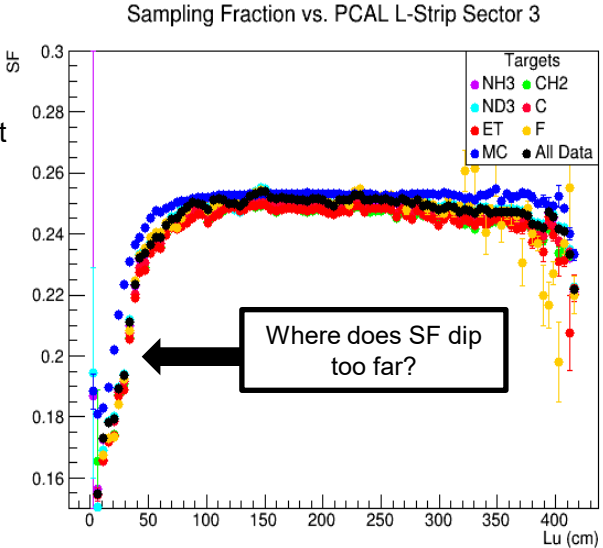
- The DC fiducial cuts based on average χ^2_{track}/NDF vs. edge variable of track
- Cuts selected qualitatively based on where average χ^2 rises relative to the rest of the distribution
- Analyzed separately for inbending and outbending data using π^+, π^-
- Tracks binned in polar scattering angle θ , momentum P
- Iterative procedure for making cuts:
 - First, make cuts for Region 3 using inbending data and cuts for Region 1 using outbending data
 - 2. After Region 1 and 3 cuts are applied, look at Region 2 and make cuts for inbending and outbending
- Checked for each sector in each region
- No momentum, θ -dependent cuts
- Vertex cuts applied
 - Summer 2022: $-9 \text{ cm} \le V_Z \le 1 \text{ cm}, |V_{X,Y}| < 2 \text{ cm}$
 - Fall 2022 & Spring 2023: -7.5 cm ≤ V_Z ≤ 2.5 cm, $|V_{X,Y}|$ < 2 cm





ECAL Fiducial Cuts

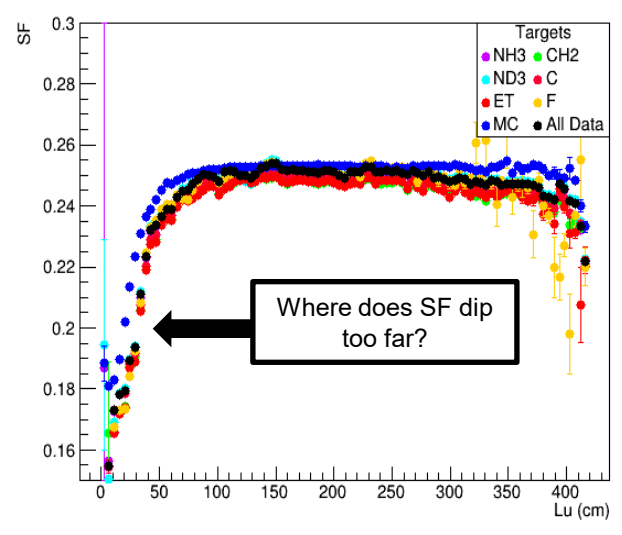
- ECAL fiducial cuts are based on the sampling fraction: energy deposited by a particle in the calorimeter
- Sampling fraction $SF = (E_{PCAL} + E_{ECIN} + E_{OUT})/P$, where E_i = energy deposited in each region of ECAL and P = momentum
- Sampling fraction is a key quantity in electron PID, since electrons have a distinguishable energy profile ($SF \approx 24\%$)
- Distinguishes electrons from minimally ionizing particles (MIPs), like π^- or π^+
- Goals of ECAL fiducial cut:
- 1. Make an "edge" cut on each region of ECAL based on where SF efficiency is lost
 - Close to the edge, the entire EM shower may not be contained, reducing SF
 - If SF is too low, it's more difficult to distinguish electrons from MIPs
- 2. Identify inefficient regions of ECAL as well as dead PMT channels
 - Make sure that inefficient regions are identified and removed
 - Check that all removed channels are cut from the Monte Carlo

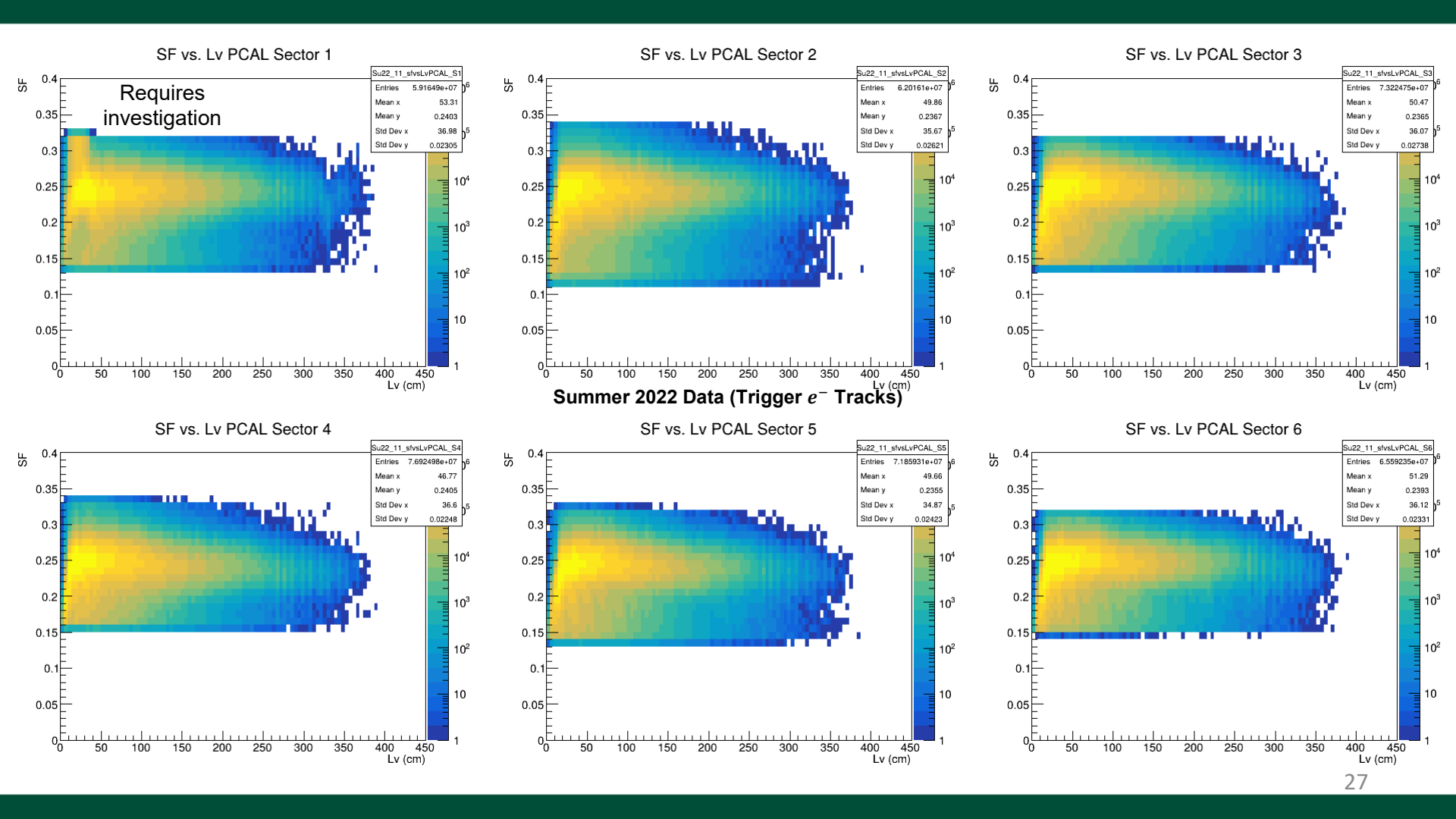


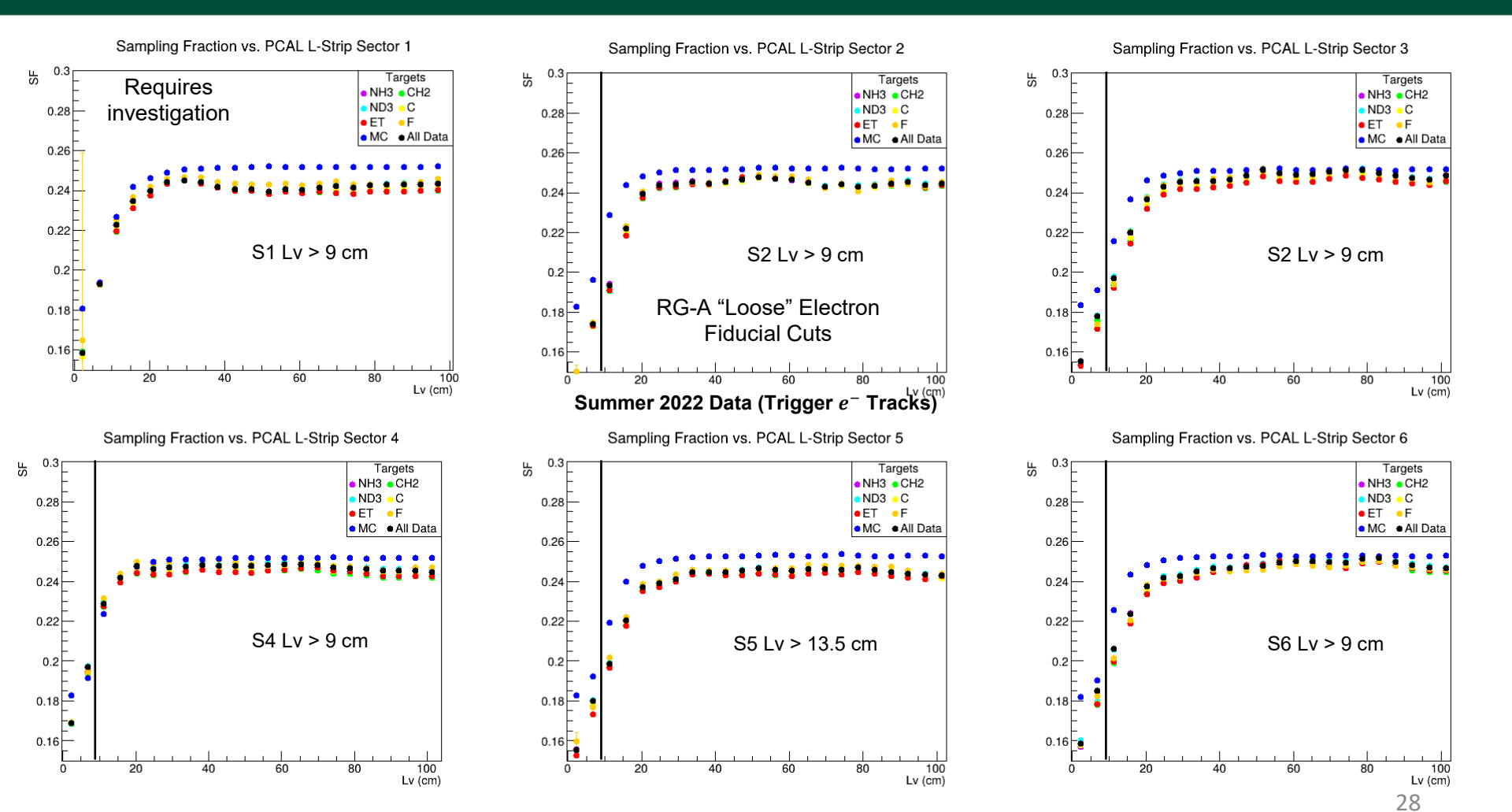
ECAL Fiducial Cuts

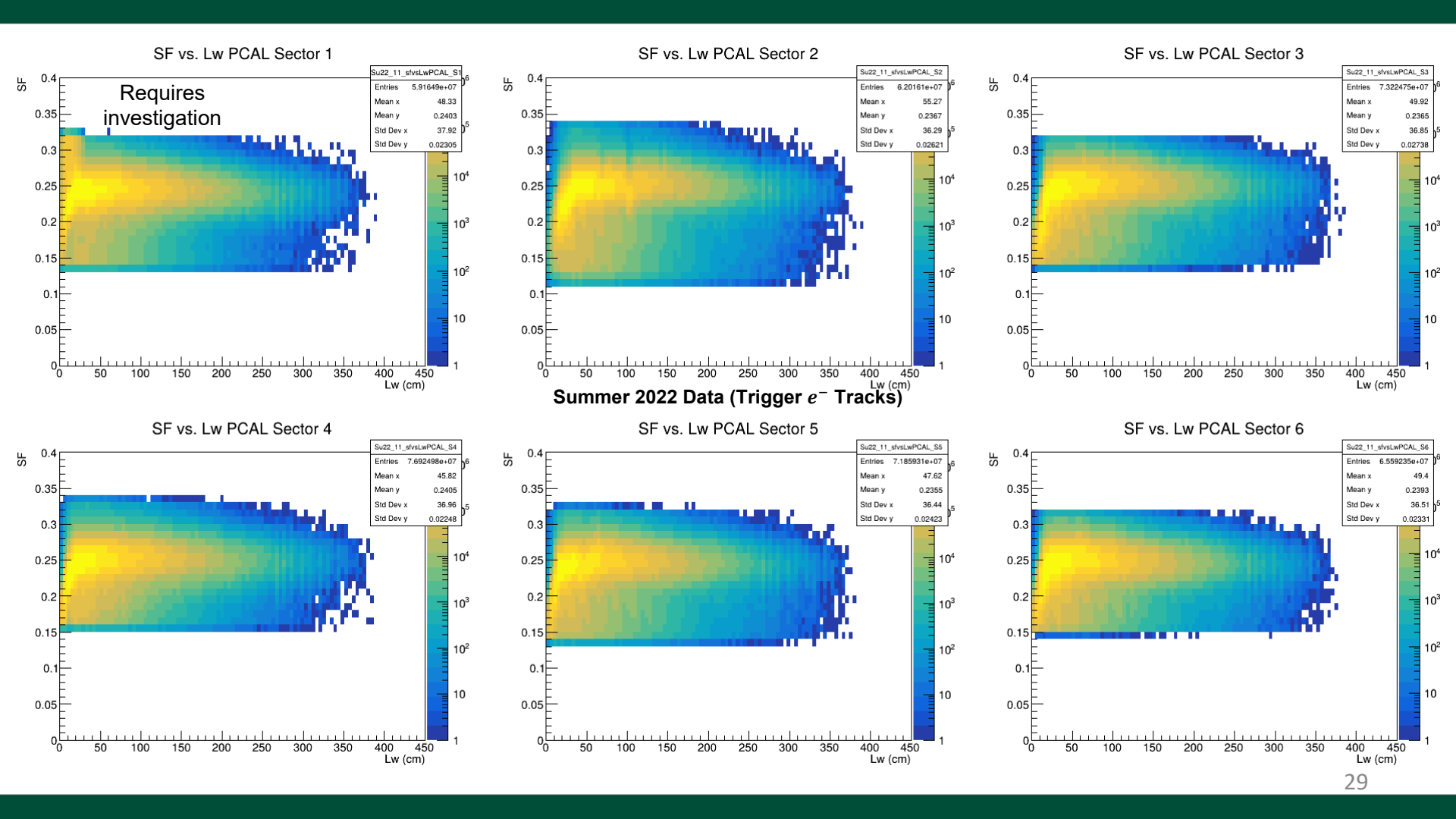
- ECAL fiducial cuts are based on the sampling fraction: energy deposited by a particle in the calorimeter
- Sampling fraction $SF = (E_{PCAL} + E_{ECIN} + E_{OUT})/P$, where E_i = energy deposited in each region of ECAL and P = momentum
- Sampling fraction is a key quantity in electron PID, since electrons have a distinguishable energy profile ($SF \approx 24\%$)
- Distinguishes electrons from minimally ionizing particles (MIPs), like π^- or π^+
- For now, I'm using the RG-A "loose" fiducial cuts for electrons in the PCAL:
 Lw, Lv > 9 cm
- More analysis is necessary for unstable SF in sector 1
- Trigger electron data only
 - My vertex cuts: $|V_{x,y}| < 2$ cm (all data sets), -8 cm $< V_Z < 2$ cm for Summer 2022, -10 cm $< V_Z < 0$ cm for Fall 2022 and Spring 2023 (needs to be updated)
 - My drift chamber fiducial cuts: EdgeR1 > 4 cm, EdgeR2 > 5 cm, EdgeR3 > 8 cm
 - Electron momentum > 2.6 GeV/c

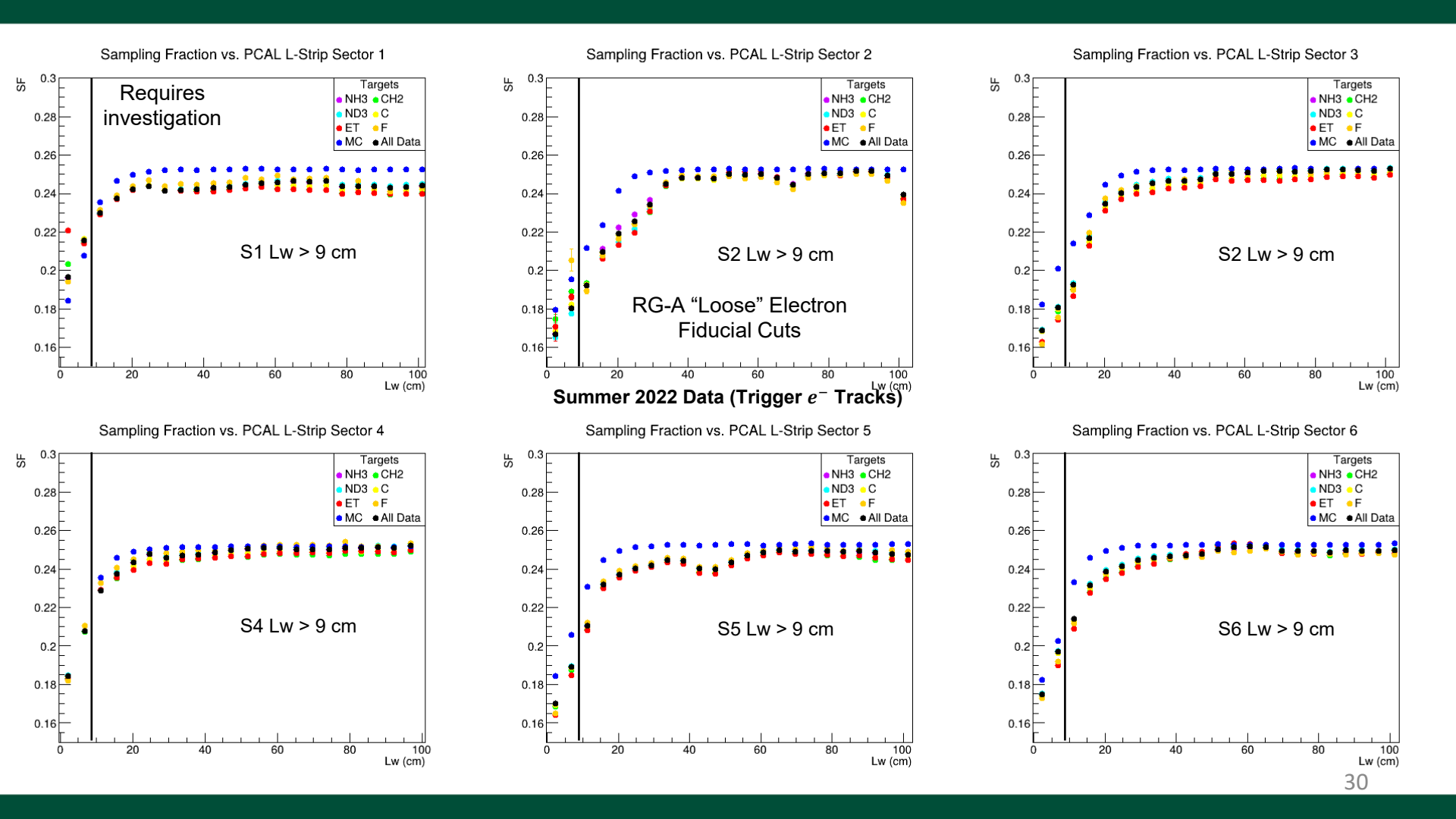
Sampling Fraction vs. PCAL L-Strip Sector 3











Thermal Contraction of Targets

- Studying the impact of thermal contraction of the target cells on the dilution factor
- Carbon, CH2, CD2 targets' geometry measured at room temperature, cooled to ~1K, so there's some contraction of target length
- Modulate the sizes of the targets as follows:

$$-\ell_C * (1 - dL_C/L_C)$$
, with $dL_C/L_C = 0.5\%$

$$-\ell_{CH}*(1-dL_{CH}/L_{CH})$$
, with $dL_{CH}/L_{CH}=2.1\%$

$$- \quad \ell_{CD} * (1 - dL_{CH}/L_{CH})$$

- L*(1-0.018) (for Teflon contraction, 1.8%)
- $\rho_C/(1 dL_{CH}/L_{CH})^3$
- $\rho_{CH} / (1 dL_{CH}/L_{CH})^3$
- $\rho_{CD}/(1 dL_{CH}/L_{CH})^3$
- ρ_A , ρ_D are unchanged

